JOURNAL OF BONE AND MINERAL RESEARCH
Volume 18, Number 11, 2003

Enamel Structure Properties Controlled by Engineered Proteins in Transgenic Mice

HANSON FONG,[1] SHANE N WHITE,[2] MICHAEL L PAINE,[3] WEN LUO,[3]
MALCOLM L SNEAD,[3] and MEHMET SARIKAYA[1]

ABSTRACT

Amelogenin protein has regulatory effects on enamel biofabrication in mammalian tooth. Using teeth obtained from transgenic mice that express two separate protein-engineered versions of amelogenins, we made structure-nanomechanical properties correlations and showed 21% hardness and 24% elastic modulus degradation compared with the age-matched wildtype littermates. We attribute the inferior properties to the disorganization of the protein matrix resulting in defective mineral formation.

Introduction: Enamel is a bioceramic initiated by the biosynthesis of a complex mixture of proteins that undergoes self-assembly to produce a super molecular ensemble that controls the nucleation and habit of the crystalline mineral phase. Ultimately, the inorganic crystals grow to almost fully replace the organic phase. This biofabrication process occurs at physiologic conditions of pH, temperature, pressure, and ion concentration and results in the hardest tissue in the vertebrate body, with the largest and longest substituted-hydroxyapatite crystals known to biomineralizing systems. The most abundant protein of forming mammalian enamel, amelogenin, has been shown to have a significant regulatory effect on this complex process.

Materials and Methods: In this work, we present the effect of protein engineering of amelogenin on the mechanical properties of the resultant mouse enamel. We have produced two types of transgenic animals that express separate versions of amelogenin proteins that lack the required self-assembly domains. The resultant matured enamel was extensively characterized for its mechanical properties at the nanoscale by means of nanoindentation and atomic force microscopy (AFM). These techniques have enabled us to probe the mechanical properties that are representative of a single enamel rod.

Results: Our nanoindentation measurements have revealed that the altered amelogenin with dysfunctional self-assembly properties resulted in a degradation by as much as 21% in hardness and 24% in elastic modulus compared with the age-matched wildtype littermates. Furthermore, the enamel formed by these defective proteins is found to display a decrease in indentation surface pile-up volume by up to 32%.

Conclusions: We attribute these inferior mechanical properties for the enamel grown by the engineered amelogenins to result from the disorganization of the nanospheres formed in the protein matrix starting at the mineral nucleation stage with a consequential alteration to the fully grown mineral component. By engineering the properties of proteins that contribute to the nanoscale level of hierarchy in enamel biomineralization, it is possible to regulate the properties of the resulting bioceramic at the mesoscale level of the tissue.

J Bone Miner Res 2003;18:2052–2059

Key words: **amelogenin, dental enamel, nanoindentation, mechanical properties, transgenic mouse, nanohardness, elastic modulus**

INTRODUCTION

DENTAL ENAMEL IS one of the most durable bioceramics produced by a vertebrate animal, being used to perform mastication throughout a lifetime. Enamel biomineralization begins with inner enamel epithelium-derived ameloblast cells secreting an extracellular protein matrix onto the mineralized dentin surface at a specialized union of dentine and enamel called the dentine-enamel junction (DEJ). A complex mixture of enamel proteins is secreted by ameloblasts that are composed of amelogenin and nonamelogenin proteins, with amelogenin being the most abun-

The authors have no conflict of interest.

[1]Department of Materials Science and Engineering, University of Washington, Seattle, Washington, USA.
[2]School of Dentistry, University of California, Los Angeles, California, USA.
[3]Center for Craniofacial Molecular Biology, School of Dentistry, University of Southern California, Los Angeles, California, USA.

dant (80–95%).[1–5] Several lines of investigation point to a role for amelogenin to control the habit of carbonated hydroxyapatite (Hap).[1,2,4–6] The amelogenin null mouse confirms the postulate that amelogenin is not required for mineral initiation,[7] but functional amelogenin protein is required to control the habit of the Hap crystallites and their organization into a fibrous continuum. In mice, the predominant mature amelogenin contains 180 amino acids,[4,8,9] although alternative splicing[7] and protein processing[10] are responsible for increasing the complexity of the enamel extracellular matrix. Strikingly, amelogenin amino acid sequence is highly similar among human, bovine, pig, and mouse, a finding that suggests common functional motifs among these species.[4]

Amelogenin has been shown to undergo self-assembly to form nanospheres in vitro and in vivo.[1,2,4–6] Transmission electron microscopy (TEM) studies have shown that these nanospheres align along the length (*c* axis) of mineralized crystals.[1,2,4–6] It is further demonstrated that there are two domains, namely domain A (residues 1–42) and domain B (residues 157–173), that control the self-assembly behavior of the nanospheres[1,2,4,6] and that these self-assembly domains are shared among amelogenins from diverse species. From in vitro studies, engineered recombinant amelogenin proteins with an A-domain deletion were observed to form smaller nanospheres, whereas those with a B-domain deletion were found to cause agglomeration of nanospheres.[1,2,6,11] Likewise, in vivo studies have also demonstrated the same trend observed in vitro among engineered amelogenins lacking the A- or B-domain based on TEM observations of a newly secreted enamel organic matrix in developing incisors.[4] Such disruption of the nanosphere assembly resulted in less ordered enamel crystallites at the nanoscale and the loss of rod-interrod boundaries at the mesoscale. Consequently, the developing enamel microarchitecture is significantly altered compared with nontransgenic age-matched control incisors. Because the loss of self-assembly domains for amelogenin induces morphological change in the growth behavior of enamel, the mechanical properties are also expected to change.

Indentation is a nondestructive method of characterizing mechanical properties of materials.[12,13] With the advent of continuous depth sensing and low force sensitivity, it is now routine to measure mechanical properties at the submicrometer scale.[14] Indentation studies on dental enamel have provided insights into dental enamel materials properties and behavior under mechanical loading. Microindentation measurements have shown that crack propagation tended to travel through the thickness of bovine enamel and arrested in the dentine-enamel junction (DEJ) zone.[15,16] Recently, White et al.[17] have shown human enamel was significantly tougher than geological apatite and that the anisotropy was lower than previously thought, indicating a high complexity in the three-dimensional (3-D) organization of enamel rods achieved by biological influences. Nanoindentation measurements by Willems et al.[18] compared the hardness between enamel and commercial dental restorative materials and revealed that the measurements on restorative materials compared well with those of the enamel values. Nanoindentation measurements achieved using a stiff cantilever-type indenter made it possible to compare intertubular and peritubular dentine, an experimental strategy that requires submicrometer spatial resolution.[19] Previous work by Fong et al. and others[20–22] mapped the hardness and elastic modulus across the DEJ, with a spatial resolution in the order of submicrometers. It was found that the DEJ zone in human incisors exhibited continuous change over a range of as wide as 15 μm.[20–22] The smooth transition of the elastic modulus through the DEJ zone is postulated to be one of the reasons for enamel longevity. Delamination does not occur despite the microcracks that are introduced during the lifetime of the tooth.[4,22]

It is evident from these studies that nanoindentation is a technique that is useful to directly obtain information on the micromechanics of biofabricated tissues, which is otherwise impossible to obtain using other methodologies. In this study, we used a transgenic approach to modify the gene expression profiles for ameloblasts and to test the hypothesis that engineered amelogenin protein, lacking self-assembly domains and previously demonstrated to perturb nanoscale and mesoscale properties for enamel, would similarly influence the mechanical properties of the biofabricated enamel. Furthermore, through the use of atomic force microscopy (AFM), a technique permitting spatial resolution at the nanometer level, we sought to accurately quantify the deformation changes taking place in the enamel of transgenic mouse incisors when subjected to indentation compared with nontransgenic age-matched controls.

MATERIALS AND METHODS

Creation of transgenic animals and sample preparation

Transgenic mouse lines were established, characterized, and maintained as unique lines according to previously published methods.[4] As before, three types of experimental enamel tissue from incisors were investigated: nontransgenic age-matched control littermates or transgenic enamel created with the contribution of amelogenin lacking the self-assembly A-domain (M180ΔA-FLAG, deleted amino acid residues 1–42) or enamel created from the contribution of amelogenin lacking the self-assembly B-domain (M180ΔB-HA, deleted amino acid residues 157–173). The procedure for breeding the transgenic mice and the analysis of transgene status was previously described.[4] The incisor teeth at 6 weeks of age were extracted from surrounding bone and stored intact in 5% PBS thymol solution at 4°C until analyzed.

Sample preparation for nanoindentation

Only lower left incisors were used for nanoindentation measurements. To ensure consistent rod orientation for every tooth, a sample preparation procedure was standardized. All teeth were mounted in epoxy parasagittally and ground with 600 grit emery paper to one-half the original tooth width. The thickness and evenness were monitored by a caliper with an accuracy of ± 25 μm. They were polished sequentially using water base polycrystalline diamond slurry with grit sizes of 6, 1, and finally 0.05 μm. There was less than 25 μm of change in thickness after the polishing step. It was established by scanning electron microscopy (SEM; JEOL 5200; JEOL, Inc, Peabody, MA, USA) exam-

ination of nine etched specimens, three from each transgenic line, that the rod orientation was consistent from tooth to tooth regardless of mouse line. (The specimens examined by SEM were not used for nanoindentation.) The final root means square (rms) roughness was within 5 nm in a given 10 μm by 10 μm area as measured by AFM (Nanoscope III with MMAFM; Veeco Instruments Inc, Santa Barbara, CA, USA).

Nanoindentation

Two types of nanoindentation studies were carried out: one using a "blunt" Berkovich diamond indenter for hardness and elastic modulus measurements, the other, using a "sharp" cube corner indenter for pile-up measurements. The pile-up measurement is a method of characterizing the enamel substance displaced to the surface after an indentation. To minimize composition change and drying, all nanoindentation measurements were performed immediately after polishing and were completed within the first 45 minutes. For measurements carried out with the Berkovich indenter, lower left incisors were extracted from (1) M180ΔB-HA transgenic mice or (2) M180ΔA-FLAG transgenic mice or (3) nontransgenic age-matched littermates, and 10 incisors from each group were tested. The indentation setup was a Hysitron Triboscope (Hysitron, Inc., Minneapolis, MN, USA) attached to a Park Autoprobe CP SPM system (Veeco Instruments Inc., Santa Barbara, CA, USA). The tip area function and stiffness were calibrated according to a procedure described by Oliver and Pharr.[14] All measurements were taken from the region that is approximately 2 mm distal to the tip of the incisor so that only the matured enamel was characterized. The hardness and reduced elastic modulus of the enamel rods were measured using a load of 1350 μN. This load was small enough to induce an indentation footprint with the projected area one-third of that of the cross-section of an enamel rod (around 3 μm). To ensure that indentations were made on the rods and that the measurements were not affected by rod boundaries, a procedure of locating the center of the enamel rods was carried out. Indentations were first made at various distances and angles from each other to enrich for indentations made in rods. When the indentation with the highest hardness value was identified, the subsequent indentations for the data set were made ~3 μm away. At least 20 indentations were made on each tooth with a total of over 200 measurements for each transgene line. Hardness and elastic modulus measurements for each transgenic group were compared with the wildtype by the *F*-test of significant variances between two populations.

For pile-up measurements, additional incisors were used—five nontransgenic age-matched littermate controls, four M180ΔA-FLAG mice, and four M180ΔB-HA mice. The same sample preparation method and indentation apparatus as described above were used. The pile-up evaluation was a three step process: (1) induce pile-up by nanoindentation, (2) characterize the pile-up debris by scanning the indents by AFM, and (3) lightly etch the specimens and scan again by AFM to reveal the relative positions of rod and indents. Indentations were made with a "cube corner" diamond tip under a load of 1000 μN. Because the apical angle of the cube corner tip was sharper, indentation stress intensity was higher compared with that of the Berkovich tip. Hence it was possible to generate a measurable "pile-up" of debris even at a lower applied load. The residual footprints that resulted from these indentations were characterized separately with a Digital Instrument (DI) Nanoscope III with MMAFM (Veeco Instruments Inc., Santa Barbara, CA, USA) using a silicon nitride cantilever tip in contact mode. This approach ensured accurate measurements of the surface features generated by the indentations. The pile-up was analyzed by performing a bearing analysis, which was available as part of the DI Nanoscope III image processing software. From a height image, which is a measurement of topographical variation on the sample surface, a reference height was chosen so that the solid volume, surface area, projected area, and height distribution could be calculated by the bearing analysis. Particular to our pile-up analyses, the polished sample surface was chosen as the reference plane. The solid volume and projected area around the indent were determined above that reference plane and referred to as "pile-up volume" and "pile-up area."

After pile-up measurements, an additional step of validating indents was carried out. To select pile-up measurements only made on enamel rods, after recording the AFM scan for bearing analysis, the same samples were subsequently lightly etched with 0.02% aqueous nitric acid, with the intention to enhance the rod boundaries while retaining the indentation footprints. The etched samples were imaged again by contact mode AFM for the sole purpose of revealing the position of the indents with respect to the physical locations of the enamel rods. Indents that were within or near the interrod (e.g., at the edge of the enamel rods) were discarded from the analysis.

To further determine the cause of the pile-up event, additional indentation tests were performed. After the pile-up was induced by an indentation, subsequent indentations were performed on the pile-up debris itself. The aim of this experiment was to determine whether the pile-up was caused by material flow or subsurface cracks. A collapse of the debris on indentation would indicate the presence of a subsurface crack, whereas a steady deformation of the debris would indicate material flow. As a comparison, the same test was conducted on two reference materials: geological apatite (brittle with observable subsurface cracks) and aluminum (ductile with no observable subsurface crack). Geological apatite and aluminum were loaded at 1800 and 400 μN, respectively, to achieve a nominal maximum depth of 200 nm, comparable with that obtained in all three mouse lines at 1000 μN.

RESULTS

Representative images of mature enamel from an incisor are shown in Fig. 1. Figure 1A is a parasagittal view of an incisor, a representative orientation for all the incisors that were prepared for nanoindentation. A typical enamel rod orientation/pattern as prepared by our standard polishing procedure is shown in Fig. 1B. A decussating pattern is clearly apparent with the end on-face of the rods tilted approximately 30° from the exposed surface. This rod orientation was observed in all the specimens examined by SEM.

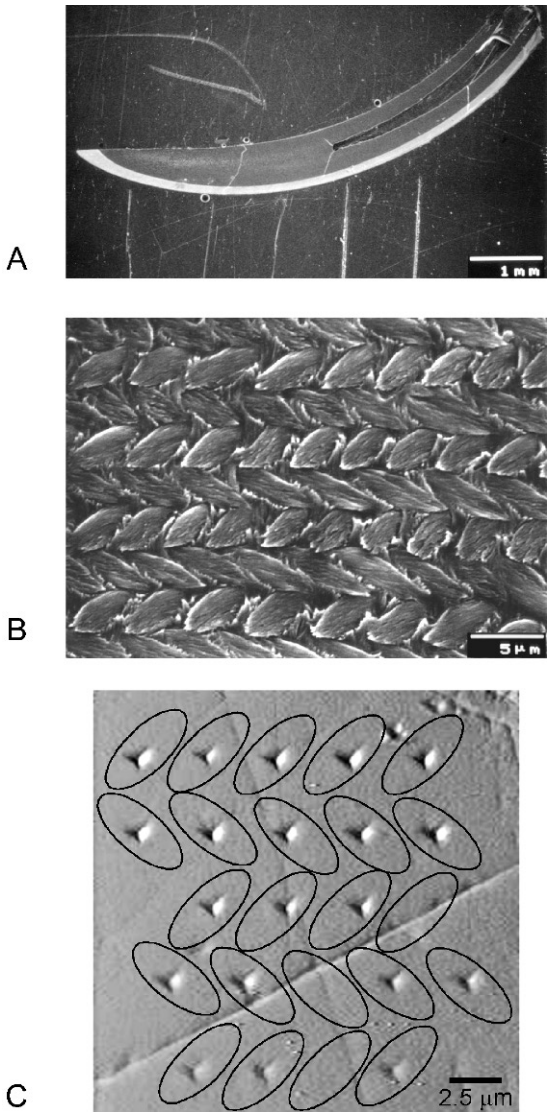

FIG. 1. Orientation images for enamel rod measurements. (A) The relative orientation for all specimens mounted for nanoindentation. (B) An SEM image represents the microstructure ground to one-half the original thickness. The decussating rod pattern, typically seen in rodent, is clearly revealed. (C) An example of nanoindentation pattern positioned to match with the individual enamel rods in the mouse tooth. The sample preparation was the same as that shown in A and B. The elliptical outlines are possible boundaries of the enamel rods based on the SEM microstructures seen in B.

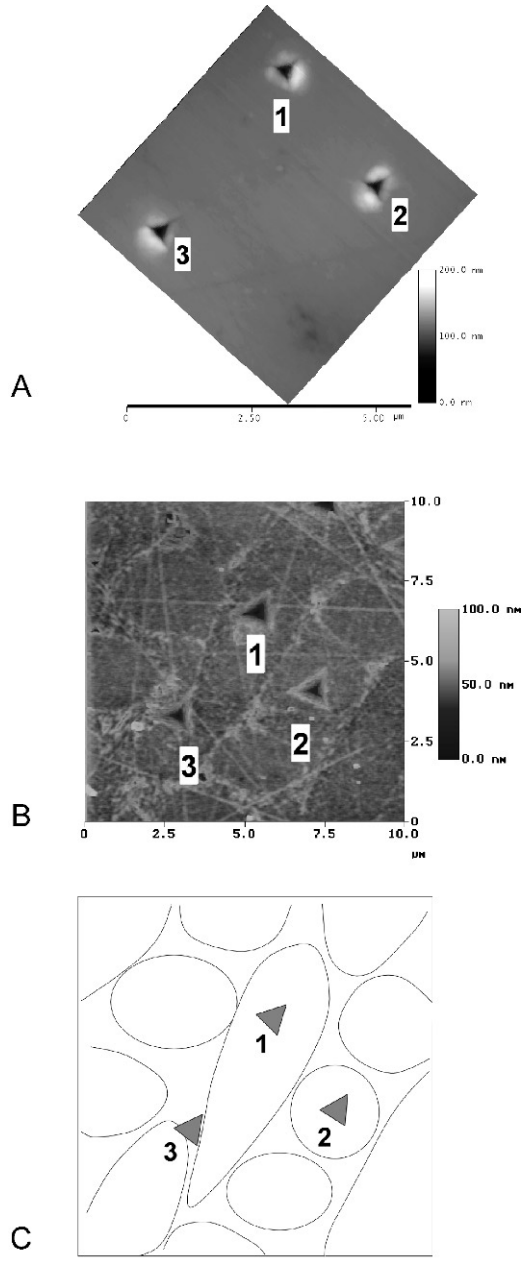

FIG. 2. AFM imaging of indentation positions for pile-up analysis. (A) Indents with surface pile-up. (B) The same indentation footprint with respect to the rod boundaries after etching. It is noted that etching also accentuated the polishing marks (straight lines). Outlines of the rods and indents are shown in C. Footprints 1 and 2 are well within the rods. Footprint 3 falls on the rod boundary. Footprints, such as 3, were excluded from pile-up analysis.

Hardness measurements were performed in such a manner that the characteristics for a rod cross-section were achieved. A representative example of a series of indentations following the procedure described in the "Nanoindentation" section with proper spacing resulting in measurements of the rod, exclusive of interrod, is presented in Fig. 1C and Fig. 2C. The average values of the hardness and elastic modulus from each experimental group are shown in Table 1. Also shown in Table 1 are the critical parameters results from the *F*-test of each transgenic group compared with the control. In each *F*-test, significant differences in the hardness and elastic modulus were found, indicating that the engineered amelogenin transgene does contribute to inferior mechanical properties for the enamel. The M180ΔA-FLAG transgenic type of enamel exhibits approximately 22% lower hardness and 24% reduced elastic modulus than the nontransgenic type. Also, as shown in the data of Table 1, the mechanical property differences between enamel from a nontransgenic littermate controls and enamel derived from a M180ΔB-HA transgenic are 8% in hardness and 18% in elastic modulus. These data reflect that the engineered de-

TABLE 1. HARDNESS AND ELASTIC MODULUS CHARACTERIZED BY USING A BERKOVICH DIAMOND TIP

	Hardness (GPa)	*Elastic modulus (GPa)**
Nontransgenic (wildtype control)	4.13 ± 0.21	105.3 ± 7.8
M180ΔA-FLAG	3.24 ± 0.33	80.2 ± 8.1
F-test against wildtype control	$p < 0.01$	$p < 0.01$
M180ΔB-HA	3.81 ± 0.27	86.2 ± 4.4
F-test against wildtype control	$p < 0.01$	$p < 0.01$

Total numbers of measurements from each group in the *F*-tests were wildtype controls, 205 over 10 incisors; M180ΔA-FLAG, 223 over 10 incisors; and M180ΔB-HA, 216 over 10 incisors.

* This is the reduced elastic modulus, measured by nanoindentation.[14]

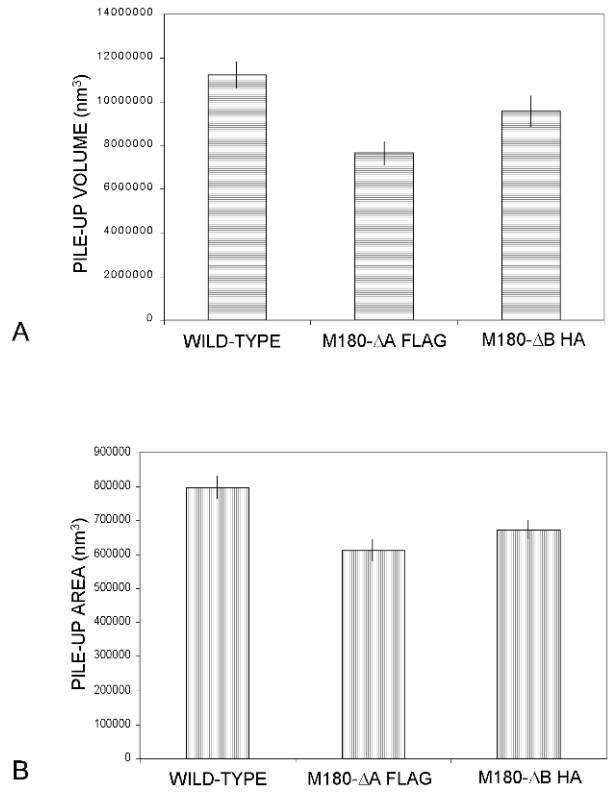

FIG. 3. Histograms of the analysis of rod indentations and resulting pile-ups. The volumetric relief, "pile-up volume," from the background surface of all individual indents positioned on the rods were integrated by bearing analysis and averaged for each group of experimental samples. The projected area of the pile-up was also quantified and designated as "pile-up area." (A) The pile-up volume found in controls, M180ΔA-FLAG, and M180ΔB-HA are, respectively, 1.12 ± 0.07, 0.76 ± 0.08, and 0.95 ± 0.08 10^7 nm^3. (B) The pile-up area found in controls, M180ΔA-FLAG, and M180ΔB-HA are, respectively, 7.98 ± 0.42, 6.12 ± 0.32, and 6.76 ± 0.37 10^5 nm^2.

fect in amelogenin self-assembly alters nanosphere function and ultimately results in defective mechanical properties in the fully grown enamel.

The extent of the pile-up debris after indentation to the enamel was determined by performing a post-indentation scan using AFM as described in the "Nanoindentation" section. The debris pile-up near the indentation is an indication of deformation behavior of a particular sample upon indentation. Hence, the debris pile-up from indentations to enamel was quantified by the height images obtained from the AFM scan of the field. These scans were first plane fitted, then the volume and area for the resulting debris pile-up were determined by bearing analysis. The location of the indentations with respect to the underlying microstructure was identified from AFM images of the indents after acid-etching the sample to permit the boundaries of the of enamel rods to be identified. Representative examples of the indentations and resulting debris fields are shown in Fig. 2. Because the acid etches rod boundaries more than the rods themselves, the location of the indents were easily identified in the resulting AFM images. Before etching (Fig. 2A), the indentations occur on a highly flat surface, and the outline for each rod boundary is not easily identified. However, after etching, the outline of the rod boundary can be identified in the height image shown in Fig. 2B, as depicted in the schematic shown in Fig. 2C. It is also noteworthy that the abrasion marks produced by polishing are likewise accentuated by etching. The results from indentations and the consequential debris field were compiled for enamel from incisors derived from at least four animals from each of the three groups (age-matched wildtype controls, M180ΔA-FLAG, and M180ΔB-HA).

The results of the pile-up analyses are presented in Fig. 3. As shown in Fig. 3A, the volume of the pile-up debris identified between nontransgenic controls and A-domain amelogenin deletion (M180ΔA-FLAG) corresponds to a 37% difference. Moreover, Fig. 3A identified a 21% difference between nontransgenic controls and deleted B-domain amelogenin (M180ΔA-FLAG). Similarly, the area corresponding to the debris pile up was obtained (Fig. 3B), and a 28% decrease in enamel from A-domain deleted amelogenin (M180ΔA-FLAG) and a 23% reduction in area for B-domain deleted amelogenin (M180ΔB-HA) were observed in the transgenic group compared with age-matched nontransgenic controls. The aforementioned differences for all of the pile-up data were found to be significant as determined by *F*-test, where each of the transgenic mouse lines was tested against the wildtype, with a confidence level of $p < 0.01$.

To determine the pile-up mechanism of the mouse teeth, a comparison was made with a brittle geological apatite (single crystalline) and a ductile aluminum (polycrystalline). On induction of a pile-up zone in geological apatite by the initial indentation, a subsequent indentation made on the pile-up debris revealed a collapse of the debris (Figs. 4A and 4B), indicating that the pile-up was created by a subsurface crack. No such collapse was observed in the aluminum (Figs. 4C and 4D), and no such collapse was observed in the biofabricated hydroxyapatite (Hap) from the mouse teeth (Figs. 4E and 4F). These observations were reproducible for 35 measurements in each material with no discernible variance within each material set.

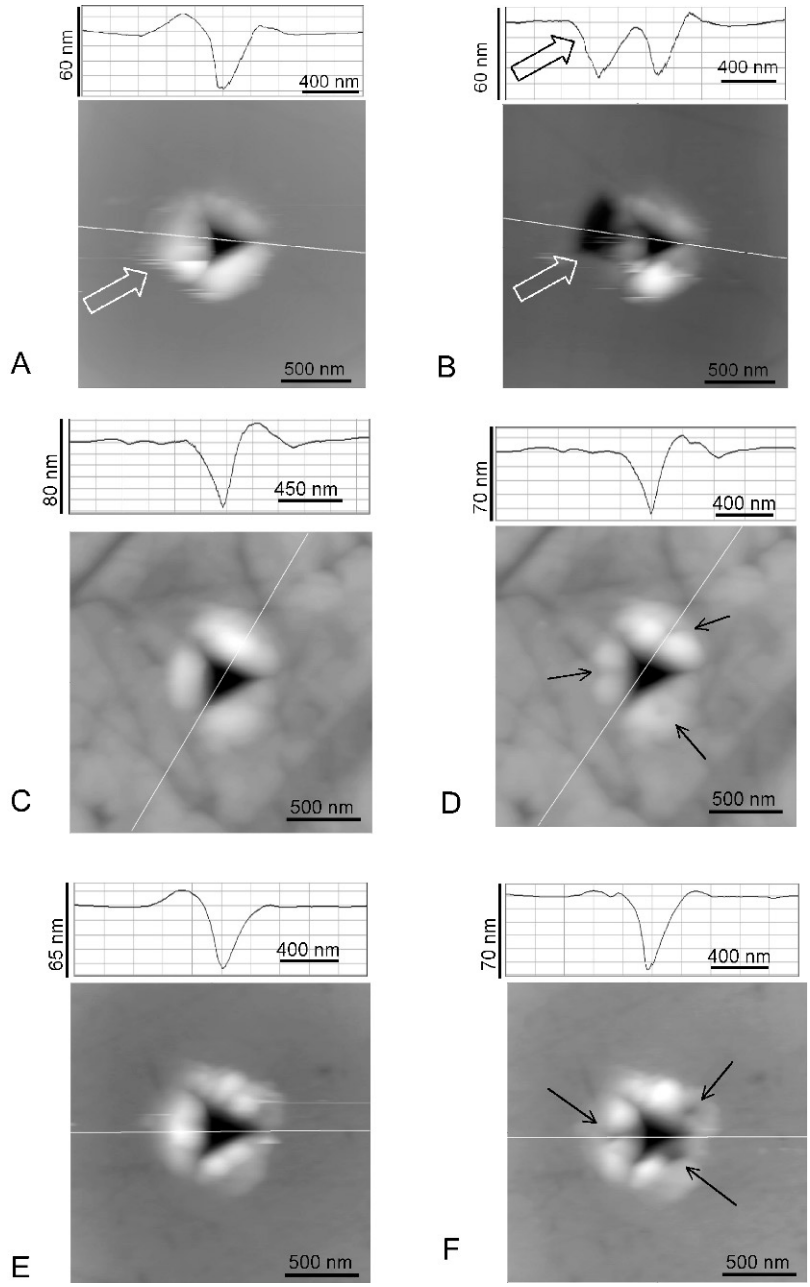

FIG. 4. Topographic profiles of the "pile-up region" for selected materials. Profiles for geologic apatite, (A and B) single crystal 001 face, (C and D) aluminum, and (E and F) biofabricated enamel Hap (A, C, and E) before and (B, D, and F) after indentation in the pile-up region were obtained. A, C, and E reveal pile-ups in all three materials. After indenting the pile-up debris, a typical subsurface crack is revealed in the geological apatite as evident by the collapse of the pile-up as shown in B. The pile-up where the collapse occurred is indicated by open arrows in A and B. The pile-up found in biofabricated enamel Hap is typically resulted from material flow, similar to ductile aluminum, as opposed to subsurface cracks. As shown in D and F, no collapse of the pile-up debris is found in (D) aluminum or (F) biofabricated Hap. Arrows in D and F indicate where subsequent indentations were made after the pile-up was created. No collapse of the pile-up debris was found in either wildtype or transgenic enamel. Shown in E and F is an example from the wildtype.

DISCUSSION

Enamel is a hierarchically ordered bioceramic tissue, and as a consequence, alteration at the nanoscale level of protein assembly results in alteration to upper orders of tissue organization. Thus, the hierarchical architecture of enamel is dependent on the ability of the organic matrix to self-assemble into a supramolecular complex that is competent to direct its own replacement by the mineral phase. It has been shown, both in vitro and in vivo, that normal amelogenin proteins form nanospheres approximately 20 nm in diameter that are aligned along the 001 direction of the Hap crystals, that is, the growth direction.[2,4] As Hap crystals continue to grow, the nanospheres decrease in size and finally disappear when mineral replacement of the organic matrix is completed. Previous studies of enamel formed by transgenic animals bearing the A-domain deleted amelogenin protein (M180ΔA-FLAG) revealed that the nanosphere size decreased to an average of 13.8 nm.[4] Similar reduction in nanosphere sizes was seen with this engineered M180ΔA-FLAG amelogenin protein produced by recombinant techniques during in vitro studies using AFM and dynamic light scatter analysis.[2] In the case of the transgenic animals bearing a deletion of the amelogenin self-assembly B-domain (M180ΔB-HA), the nanospheres seem to collapse into larger size nanospheres in the newly secreted organic enamel matrix.[4] Studies carried out in vitro with the M180ΔB-HA-engineered amelogenin proteins pro-

duced by recombinant techniques corroborate the in vivo observation that the nanospheres are unstable over minutes, coalescing to form larger sized nanospheres as agglomerations with an average size of 80 nm^2. Paine et al.[4] postulated a mechanism by which defects in either of the amelogenin self-assembly domains (domain-A or domain-B) could affect the nanoscale spheres with hierarchical impact adversely altering the rod and interrod boundaries. Additional studies suggest that the misassembled nanospheres alter the habit of the Hap, allowing crystallites to lose registration with one another and resulting in a more randomized orientation of crystallites.[4,23] We suggest that the competency of the enamel organic extracellular matrix to direct replacement by the mineral phase was adversely altered by the engineered amelogenin. The changes in the self-assembly properties of the predominant protein of the enamel matrix has compromised the creation of the inorganic phase, and thus, altered the mechanical integrity both within a given enamel rod (this study) and among a group of enamel rods.[4]

The nanomechanical tests described here were carried out to further investigate how the altered structure affected the mechanical properties within an enamel rod. The nanoindentation measurements have demonstrated that both transgenic mouse lines resulted in significant decrease in hardness and elastic modulus. However, hardness and elastic modulus values alone cannot reveal the mechanism that caused the decrease in the transgenic lines. A better insight into the structure-property relationship may be found by correlating the deformation behavior of the structure with that of the forces used to generate the nanohardness measurements. This is performed by quantifying deformation behavior in a material by characterizing the debris "pile-up" that forms with each indentation as a result of surface displacement of the test material by the indenter.

There are two possible reasons for the higher pile-up volume observed in the nontransgenic group. First, mineral density is greater, meaning there is less space available in the surrounding tissue, which the indented volume can deform into by means of compaction. Second, the nontransgenic group exhibits subsurface cracks, whereas the transgenic groups exhibit less or no subsurface cracks. Such cracks originate from the side of the indenter tip and propagate radially outward. Because the crack creates a gap between material displaced below the sample surface and the bulk, the pile-up field would appear larger than it really is. It is hypothesized that if subsurface cracks were present, indenting on the pile-up field would cause it to collapse. Such an experiment was conducted on the mouse enamel samples as well as on a single crystal of geological apatite (in the latter, the 001 crystallographic plane was tested) and aluminum. Geological apatite represented a fully dense, brittle mineral where indentation cracks would be expected. Aluminum represented a ductile material where only plastic flow would be expected. The pile-up zones around the first indentations were subsequently indented a second time. Images of before and after indenting the pile-up zones were acquired using the same cube-corner tip. As seen in images shown in Figs. 4A, 4C, and 4E, all materials exhibit significant pile-up volumes. However, collapse of the pile-up structure is only observed in geological apatite, suggesting that large pile-up volume is caused by the presence of subsurface cracks. Wildtype or engineered enamel and aluminum metal, on the other hand, exhibit no collapse in the pile-up region, supporting the notion that the pile-up debris observed is not a result of subsurface crack in the bioceramic enamel but is due rather to material flow.

The nanoindentation measurements we made in the transgenic or wildtype mouse enamel samples characterize the mechanical properties of individual rods in the matured stage. Overall, the enamel made from wildtype amelogenin exhibits a higher hardness, as well as greater pile-up field. Knowing that pile-up volume and area is primarily the result of material flow, we argue that our observations strongly support the notion that the matured enamel, biofabricated in the presence of an engineered amelogenin defective in self-assembly to form nanospheres, has a lower mineral density than the wildtype control. The reduction in mineral density increases the tendency for the indented volume to deform through compaction, resulting in the decrease in pile-up.

In comparison with other structural materials, such as metals and ceramics, the hardness of mouse enamel is comparable with that of a mild steel and is one-half the value for geological apatite. The decrease in hardness for biologically fabricated apatite compared with geologically fabricated apatite may be attributed to the role that the organic enamel matrix plays in controlling crystal habit or by the retention of a very small residue of enamel protein among the crystallites that compose a rod or interrod. The unique deformation behavior observed in these bioceramics could, therefore, be directly related to the microstructure achieved by the enamel organic matrix.

The matrix exists to be largely, but not entirely, replaced by mineral in the mature enamel. Changes in the abundance of specific enamel proteins or defects in protein function are predicted to affect the properties of the final mineral product. Microcracks are usually the dominant deformation mechanism in apatite as well as most known brittle ceramics when a sufficient stress is introduced by indentation. However, in enamel, material flow is the prevalent deformation behavior at the size scale observed by nanoindentation. This suggests that biomineralization has changed the mechanical properties through the control of the microstructure. Mammalian enamel is not a monolithic ceramic layer, but rather consists of bundles of ceramic crystals, on the order of 50 nm wide, that are biofabricated. On indentation, sliding of these crystals become the dominant deformation mechanism rather than catastrophic cracks. For a tooth to survive long periods of mastication, it must be wear resistant. Material removal by wear can be either "molecule by molecule" or fracture in "chunks." All things being equal, the former is a slower process. Although the hardness is lower for enamel compared with mineral apatite, its structural design allows enamel to be more fracture resistant, even at the nanoscale. Therefore, material loss during wear caused by fracture is greatly reduced, prolonging the functional life of the tooth. This is another example of the ability of a biological system to synthesize a ceramic material that is optimally adapted by evolution for functional usage.

Genetically engineered changes to amelogenin protein had been shown to bring about modification to its self-assembly properties, and consequently, change to habits of

the resulting mineral that replaces it. In this study, we demonstrated that such changes also result in deteriorating mechanical properties of enamel at the micro- and nanometer scales, in particular, hardness and stiffness. The results of microstructure and nanoindentation pile-up data indicate that the reductions in hardness and elastic modulus are due to disruption of microstructure and a decrease in mineral density achieved by alteration to the enamel organic matrix.

ACKNOWLEDGMENTS

This work is supported by Grants DE-06988, DE-11704, DE-12420, DE-13045, DE-02848, DE-12350, DE-14189, and DE-13404 from the National Institute for Dental and Craniofacial Research. The authors thank Daniel Heidel for helpful discussions and assistance in sample preparation.

REFERENCES

1. Fincham A, Moradian-Oldak J, Simmer J, Sarte P, Lau E, Diekwisch T, Slavkin H 1994 Self-assembly of a recombinant amelogenin protein generates supermolecular structures. J Struct Biol **112:** 1103–1109.
2. Moradian-Oldak J, Paine ML, Lei Y, Fincham A, Snead ML 2000 Self-assembly properties of recombinant engineered amelogenin proteins analyzed by dynamic light scattering and atomic force microscopy. J Struct Biol **131:**27–37.
3. Nanci A, Ahluwalia J, Pompura J, Smith C 1989 Biosynthesis and secretion of enamel proteins in the rat incisor. Anat Rec **224:**277–291.
4. Paine ML, Zhu DH, Luo W, Bringas P Jr, Goldberg M, White S, Lei Y, Sarikaya M, Fong H, Snead ML 2000 Enamel biomineralization defects result from alterations to amelogenin self-assembly. J Struct Biol **132:**191–200.
5. Smith C 1998 Cellular and chemical events during enamel maturation. Crit Rev Oral Biol Med **9:**128–161.
6. Fincham A, Moradian-Oldak J, Diekwisch T, Lyaruu D, Wright J, Bringas P Jr, Slavkin H 1995 Evidence for amelogenin "nanospheres" as functional components of secretory-stage enamel matrix. J Struct Biol **115:**50–59.
7. Gibson CW, Yuan ZA, Hall B, Longenecker G, Chen E, Thyagarajan T, Sreenath T, Wright JT, Decker S, Piddington R 2001 Amelogenin-deficient mice display an amelogenesis imperfecta phenotype. J Biol Chem **276:**31871–31875.
8. Snead ML, Zeichner-David M, Fincham AG, Woo SL, Slavkin HC 1985 DNA sequence for cloned cDNA for murine amelogenin reveal the amino acid sequence for enamel-specific protein. Biochem Biophys Res Commun **129:**812–818.
9. Simmer JP, Snead ML 1995 Molecular biology of the amelogenin gene. In: Robinson C, Kirkham J, Shore R (eds.) Dental Enamel: Formation to Destruction. CRC Press, Boca Raton, FL, USA, pp. 59–84.
10. Moradian-Oldak J, Simmer JP, Lau EC, Sarte PE, Slavkin HC 1994 Detection of monodisperse aggregates of a recombinant amelogenin by dynamic light scattering. Biopolymers **34:**1339–1347.
11. Hunter G, Curtis H, Grynpas M, Simmer J, Fincham A 1999 Effects of recombinant amelogenin on hydroxyapatite formation in vitro. Calcif Tissue Int **65:**226–231.
12. Gilman JJ 1973 Hardness—a strength microprobe. In: Westbrook JH, Conrad H (eds.) The Science of Hardness Testing and Its Research Applications. American Society of Metals, Metals Park, OH, USA, pp. 51–72.
13. Tabor D 1986 Indentation hardness and its measurement: Some cautionary comments. In: Blau PJ, Lawn BR (eds.) Microindentation Techniques in Materials Science and Engineering, American Society of Testing and Materials, Philadelphia, PA, USA, pp. 129–159.
14. Oliver W, Pharr G 1992 An improved technique for determining hardness and elastic modulus using load and displacement sensing indentation experiments. J Mater Res **4:**1564–1586.
15. Lin C, Douglas W 1994 Structure-property relations and crack resistance at a bovine dentin-enamel junction. J Dent Res **73:**1072–1078.
16. Xu H, Smith D, Jahanmir S, Romberg E, Kelly J, Thompson V, Rekow E 1998 Indentation damage and mechanical properties of human enamel and dentin. J Dent Res **77:**472–480.
17. White S, Luo W, Paine ML, Fong H, Sarikaya M, Snead ML 2001 Biological organization of hydroxyapatite crystallites into a fibrous continuum toughens and controls anisotropy in human enamel. J Dent Res **80:**321–326.
18. Willems G, Celis JP, Lambrechts P, Braem M, Vanherle G 1993 Hardness and Young's modulus determined by nanoindentation technique of filler particles of dental restorative materials compared with human enamel. J Biomed Mater Res **27:**747–755.
19. Kinney J, Balloch M, Marshall S, Marshall G, Wehs T 1996 Atomic force microscope measurements of the hardness and elasticity of peritubular and intertubular human dentin. J Biomech Eng **118:**133–137.
20. Fong H, Sarikaya M, White S, Snead ML 1999 Nano-mechanical properties profiles across dentin-enamel junction of human incisor teeth. Mater Sci Eng C **7:**119–128.
21. Marshall GWJ, Balooch M, Gallagher RR, Gansky SA, Marshall SJ 2001 Mechanical properties of dentinoenamel junction: AFM studies of nanohardness, elastic modulus, and fracture. J Biomed Mater Res **54:**87–95.
22. White S, Paine ML, Luo W, Sarikaya M, Fong H, Yu Z, Li Z, Snead ML 2000 Dentino-enamel junctions: Broad transitional zones uniting dissimilar bioceramic composites. J Am Ceramic Soc **83:**238–240.
23. Dunglas C, Septier D, Paine ML, Zhu DH, Snead ML, Goldberg M 2002 Ultrastructure of forming enamel in mouse bearing a transgene that disrupts the amelogenin self-assembly domains. Calcif Tissue Int **71:**155–166.

Address reprint requests to:
Mehmet Sarikaya, PhD
University of Washington
Materials Science and Engineering Department
302 Roberts Hall, Box 352120
Seattle, WA 98195, USA
E-mail: sarikaya@u.washington.edu

Received in original form September 30, 2002; in revised form June 13, 2003; accepted July 16, 2003.